AD-A133 575 HIGH PRECISION MATERIAL STUDY AT NEAR MILLIMETER WAVELENGTHS(U) NORTH CAROLINA CENTRAL UNIV DURHAM NC DEPT OF PHYSICS J M DUTTA ET AL. 30 AUG 83 1/1

UNCLASSIFIED ARO-17775.3-PH-H DAAG29-80-G-0005 F/G 20/6 NL

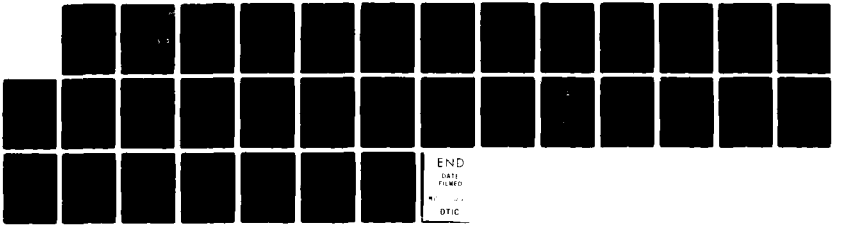

END

DATE FILMED

DTIC

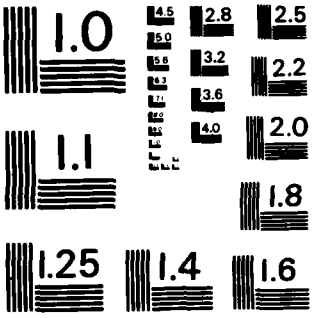

AD-A133 575

ARO 17775.3-PH-H

SECURITY CLASSIFICATION OF THIS PAGE (When Data Entered)

REPORT DOCUMENTATION PAGE

READ INSTRUCTIONS BEFORE COMPLETING FORM

1. REPORT NUMBER: Final Report	2. GOVT ACCESSION NO.
3. RECIPIENT'S CATALOG NUMBER	
4. TITLE (and Subtitle): High Precision Material Study at Near Millimeter Wavelengths	5. TYPE OF REPORT & PERIOD COVERED: Final Report 9-10-80 - 9-9-83
	6. PERFORMING ORG. REPORT NUMBER: N.C. Cent. Univ., Phys. Dept.
7. AUTHOR(s): Dr. Jyotsna M. Dutta and Dr. C. R. Jones	8. CONTRACT OR GRANT NUMBER(s): DAAG29-80-G-0005
9. PERFORMING ORGANIZATION NAME AND ADDRESS: Department of Physics, North Carolina Central University, Durham, NC 27707	10. PROGRAM ELEMENT, PROJECT, TASK AREA & WORK UNIT NUMBERS
11. CONTROLLING OFFICE NAME AND ADDRESS: U. S. Army Research Office, Post Office Box 12211, Research Triangle Park, NC 27709	12. REPORT DATE: August 30, 1983
	13. NUMBER OF PAGES
14. MONITORING AGENCY NAME & ADDRESS (if different from Controlling Office)	15. SECURITY CLASS. (of this report): Unclassified
	15a. DECLASSIFICATION/DOWNGRADING SCHEDULE

16. DISTRIBUTION STATEMENT (of this Report)

Approved for public release; distribution unlimited.

DTIC ELECTE OCT 12 1983 D

17. DISTRIBUTION STATEMENT (of the abstract entered in Block 20, if different from Report)

18. SUPPLEMENTARY NOTES

THE VIEW, OPINIONS AND/OR FINDINGS CONTAINED IN THIS REPORT ARE THOSE OF THE AUTHOR(S) AND SHOULD NOT BE CONSTRUED AS AN OFFICIAL DEPARTMENT OF THE ARMY POSITION, POLICY, OR DECISION, UNLESS SO DESIGNATED BY OTHER DOCUMENTATION.

19. KEY WORDS (Continue on reverse side if necessary and identify by block number)

Near Millimeter Waves, Optically pumped Molecular Laser, Rexolite, TPX, Dynasil 4000.

20. ABSTRACT (Continue on reverse side if necessary and identify by block number)

Various quasi-optical components for effective beam transmission at near millimeter wavelengths have been studied. A double-beam apparatus which may be configured as a Mach-Zehnder interferometer has been assembled for dielectric characterization of materials. Values of optical constants, obtained at a frequency of 245 GHz with an optically pumped laser source, are reported for several low-loss materials. The potential for improvements and increased accuracies are discussed.

DD FORM 1 JAN 73 1473 EDITION OF 1 NOV 65 IS OBSOLETE

Unclassified

SECURITY CLASSIFICATION OF THIS PAGE (When Data Entered)

DTIC FILE COPY

83 10 12 141

TABLE OF CONTENTS

LIST OF ILLUSTRATIONS

LIST OF TABLES

Abstract

A simple and versatile instrument for the measurement of optical constants in the near millimeter spectral region is described. Studies of quasi-optical components used for effective beam transmission and control in this instrument are reported. These studies include transmission characteristics of dielectric waveguides and performance of a variable coupler based on frustrated total internal reflection. Operation of this instrument as a two-beam interferometer for determining the index of refraction or as a device to measure transmission for determining the absorption coefficient are described. Values measured with this instrument at 245 GHz, using an optically pumped molecular laser as the source, are reported for several low-loss materials. Appropriate corrections and error estimates are discussed. The potential for improvement and increased accuracies are discussed.

I. Introduction

There is a growing interest in potential applications for radiation in the near-millimeter (NMM) region of the electromagnetic spectrum, defined roughly as radiation with wavelengths between 0.3 and 3 millimeters. These applications include, for example, spectroscopy, plasma diagnostics and imaging radar. Realization of these potential applications is often limited by the minimal amount of data which is available on the optical properties of materials at these wavelengths. A reliable, high-precision data base must be accumulated if instrumentation is to be designed with confidence.

Several factors make reliable accuracy and high precision in the measurement of optical properties difficult to attain in this spectral region. In the past, source and detector limitations have often been predominant and recent developments in source and detector technology have only partially alleviated these limitations. There are also basic problems of measurement technique arising because of the intermediate character of this radiation, which lies between the microwave and the infrared spectral regions. Typical microwave measurement techniques, which rely on systems using fundamental-mode waveguides, are prohibited by the small dimensions and high losses encountered at these wavelengths. As a result, free-space measurement techniques, referred to as "quasi-optical," are frequently employed. However, the relatively long wavelengths involved necessitate the use of large apertures and/or correction for diffraction effects.

A simple and versatile instrument designed to circumvent many of these problems is described here. This instrument utilizes the power and coherence of a laser source and combines the use of quasi-optical techniques with the introduction of over-moded dielectric waveguides to limit diffraction spreading of the radiation. The instrument can readily be configured as a two-beam interferometer for determining the index of refraction or as a device to measure transmission for determining the absorption coefficient. The versatility of this instrument derives in part from the use of a variable coupler, based on

frustrated total internal reflection. This component functions as either an adjustable beam-splitter or as a self-calibrating attenuator.

Details of the laser source, the dielectric waveguide and other components of the instrument are described in the following sections. Error sources and the attainable accuracy and precision are discussed. Values of the optical constants at a frequency of 245 GHz, where relatively little data is currently available, are presented for several representative materials.

II/ Optically Pumped Molecular Laser

The source used for these studies is generally referred to as an optically-pumped molecular laser (OPML) because the NMM lasing action derives from a molecular gas which is excited by absorption of radiation instead of by an electrical discharge (1). A diagram of the OPML is shown in Figure 1.

A grating-tuned CO_2 laser having a single-line output power of $\sim$ 25 W provides the pumping radiation. The CO_2 laser tube is of conventional design with a 1 cm bore and a 140 cm discharge length. ZnSe optics are used for the Brewster windows and the output coupler. A 150 line/mm grating provides for line selection and a piezoelectric translator gives fine tuning within the output linewidth.

The NMM cavity is formed by a dielectric waveguide of two-meter length and 44 mm bore with mirrors mounted proximate to each end (2). The input mirror is of polished copper and contains a 3 mm diameter central aperture through which the pump radiation enters the NMM cavity. The output mirror is a hybrid design on a high-resistivity silicon substrate (3). A central region of 15 mm diameter is coated with multi-layer dielectrics for high reflectivity of the pump radiation but is partially transparent at NMM wavelengths. A gold-coated annulus surrounds this central region, providing high reflectivity for both wavelengths. Pump radiation enters the NMM laser through a ZnSe Brewster window and the NMM output exists through a window of Z-cut quartz.

The CO_2 pump laser and the NMM laser are assembled in a common framework of INVAR rods to reduce thermal drifts. Active stabilization to increase the long-term stability is provided by a lock-in, feed-back system. In the present studies, measurement periods rarely exceeded 15 minutes and passive stabilization alone was found to be adequate.

This laser system has operated satisfactorily at a number of wavelengths throughout the NMM region. Typical performance with formic acid (HCOOH) as

the lasing medium yielded 25 mW of power at 393.6 micrometers when pumped with 25 W from the CO_2 laser. For the materials measurements reported here, $C^{13}H_3F$ was used as the lasing medium, producing 3 mW of power at 245 GHz with 20 W of pump power. (These NMM powers were read directly from a Scientech power meter without correction.)

The spatial mode quality of the output is an important parameter when designing apparatus to be used with this source. Figure 2 shows the spatial beam profile at the focus of a lens. The data points were obtained with a 1 mm aperture in front of a Golay cell detector. The results are well fit by a Gaussian intensity profile, hence computations based on Gaussian optics(4) can be readily used. Additional studies have confirmed a high degree of linear polarization.

It can be seen that the OPML is an ideal source in many respects. The output is a polarized, relatively powerful, Gaussian beam, well suited to the study of optical properties of materials. During these studies, the OPML was operated at a frequency of 245 GHz but it may be used for measurements at many other frequencies by utilizing the laser lines which have been tabulated (5). For example, in the range of prime interest between 150 and 400 GHz, Table I lists twelve lines which are reported to yield as much or more power than the line used in these studies. The lines listed in Table I are available from just four gases and their density corresponds to an average spacing of 21 GHz (0.7 cm^{-1}).

III. Dielectric Waveguides

Systems which function in a free-space mode at NMM wavelengths often suffer from the substantial effects of diffraction. This problem can be circumvented while maintaining modest system aperture by employing oversized dielectric waveguides as low-loss transmission lines. A series of experiments were conducted at 245 GHz to verify the suitability of using this approach in an instrument to measure optical constants.

Waveguide Modes

For this application, the maintenance of good spatial mode quality is of primary importance. Marcatili and Schmeltzer first derived the electric field configuration and propagation constants for hollow, circular, dielectric waveguides whose diameters are large compared to the wavelength (6). More recently, Steffen and Kneubühl (7) and Degnan (8) have treated this subject. There are three categories of modes which are supported by such guides: transverse electric (TE_{01}), transverse magnetic (TE_{01}) and hybrid (EH_{mm}). Of these categories, the low-order hybrid modes have the lowest losses and are most relevant for the application envisioned. In particular, the fundamental EH_{11} mode has the lowest loss and desirable spatial characteristics.

The first experiments undertaken were to verify that the free-space Gaussian mode from the OPML, as shown in Figure 2, could be effectively coupled into the waveguide, exciting only the EH_{11} mode. This coupling problem has been addressed by Abrams (9) and recently investigated by Crenn (10). Our observations confirm the prediction of Abrams , that the coupling is efficient when the beam is focused at the entrance to the guide with a waist radius of approximately 0.6435a, where a is the radius of the guide. A lens made from TPX plastic was used to focus the output of the OPML to meet this condition at the entrance to a one-meter long guide of 9.5 mm radius. It was not possible to directly monitor the mode inside the waveguide. Instead, the beam profile which occurred in free-space at a distance of 20 cm from the guide exit was examined by the same aperture/detector combination previously used. The data points obtained are shown in Figure 3. Degnan (8) has treated theoretically the coupling of an EH_{11} waveguide mode into free-space and the profile to be expected is shown on Figure 3 for comparison. The excellent agreement obtained indicates that the EH_{11} mode was predominantly excited. Careful angular alignment of the guide axis to the incoming beam was found to be necessary to avoid excitation of higher order modes. It is also noteworthy that the far-field beam profile can be

approximated by a Gaussian. This has been discussed by Belland and Creen (11) who point out that a Gaussian beam when focused to a waist and weakly diffracted by a circular aperture can be approximated in the far-field region by another Gaussian emanating from a "fictitious" waist w_0'. If the actual waist at the aperture is 0.6435a then the proper fictitious waist to use for describing the diffracted Gaussian is $w_0' = 0.5869a$. The profile measured in this experiment agrees with this approximation within ~7%.

As further confirmation that the propagation could be described as an EH_{11} mode in the guide, the expansion of the beam as it exited into free-space was studied. Figure 4 shows the measured beam radius versus the distance the wave has propagated since exiting the guide. The theoretical curve according to Degnan's theory is shown for comparison. The experimental results agree satisfactorily with the theoretical expectation for an EH_{11} mode in the guide.

Propagation Losses

A study of propagation and coupling losses was conducted by measuring transmission of a series of guides having the same diameter, 19 mm, but various lengths. The experimental arrangement for this study is shown in Figure 5. D_1 and D_2 are identical pyroelectric detectors (Laser Precision Rkp-545). D_1 monitors a portion of the output power from the OPML while D_2 measures the power transmitted by the waveguide under study. Use of a ratiometer (Laser Precision Rkp-5200) compensates for any variations in laser output during the measurement. Before recording the transmission through a particular guide, it was first carefully aligned and the exiting mode profile scanned to ensure that higher-modes were not excited. From the plot of $-\ln T$ versus waveguide length shown in Figure 6, the coupling loss and propagation loss coefficient may be determined. The coupling loss was found to be less than 2% as predicted (9). The measured propagation loss coefficient of 7×10^{-3} cm^{-1} agrees with the theory (6) within the experimental error.

A final waveguide study was undertaken to investigate the effect of introducing a free-space gap into the waveguide. This effect is of considerable importance because it is sometimes necessary to have such gaps where components or samples can be inserted.

The arrangement of Figure 5 was used with the single waveguide replaced by two colinear guides separated by a variable gap. The first guide was 1-meter in length and the second guide 20 cm in length. The power at the exit to the second guide was measured as a function of the gap length and the results are shown in Figure 7 . As expected, the power transmitted decreases as the gap is made larger. However, the decrease is quite gradual at first and spacings large enough to accomodate most components do not introduce prohibitive losses. Equally important was the observation that the beam profile at the exit of the second waveguide is quite insensitive to the dimension of the gap. Thus it can be concluded that a moderate free-space gap in the guide will cause modest power losses while having little effect on the beam profile.

Comments

The guide diameter of 19 mm chosen for these experiments is a compromise between minimizing the aperture size and avoiding excess loss and alignment difficulty with smaller guides. It is noteworthy that these experiments, in which the ratio of guide radius to the wavelength was approximately 8, agree very well with the theoretical results which were derived under the assumption that this ratio is very large.

IV. Variable Coupler/Attenuator

The types of quasi-optical components which are available for the implementation of NMM systems is quite limited. In particular, variable couplers and calibrated attenuators are not commonly available. Several researchers in the millimeter-wave region have discussed the potential versatility of a bidirectional variable coupler operating on the principle of

frustrated total internal reflection (12), (13), (14) and have demonstrated the feasibility of such a device. However, this component has seen little recent utilization. The theoretical operation of this device is readily understood by reference to Figure 8 . Two identical prisms, composed of a low-loss dielectric, are separated along a face diagonal by a small gap. The dielectric constant must be such that radiation entering port 1 is incident on the diagonal at an angle greater than the critical angle. When the gap between the prism is large, the incident radiation is totally reflected into port 2 and when the gap is closed to zero all of the incident radiation passes through into port 3. At intermediate settings, the radiation entering at port 1 is divided between ports 2 and 3 in a ratio which can be precisely controlled by the setting of the gap size.

Figure 8 shows a plot of the ratio of the power at port 2 to the power at port 3 as a function of the prism separation. This data was taken at 245 GHz with the prism separation determined by a stepping-motor driven micrometer. The power ratio was measured with the same detector-ratiometer combination used for the waveguide studies. For comparison, a curve is shown corresponding to the theoretical equations from reference (13). The performance of this device is generally in good agreement with theoretical expectations. This agreement also suggests that the detector linearity is good over the dynamic range used. Two minor deviations from ideality are evident. First, at very small prism separations, imperfections in the prism surfaces and/or their alignment prevent the attainment of zero separation and cause the data to deviate. Secondly, small oscillations of the data about the theoretical curve can be attributed to reflections at the prism faces. Over the range from -5dB to +15dB, the average deviation is less than 0.2dB. This can be reduced, if necessary, by including reflection effects in the calculations (15). Further studies have also confirmed that a Gaussian beam entering this device is divided into two Gaussian beams with no mode distortion.

For the development of NMM instrumentation this has proven to be a very useful beam-control component. It can function as an adjustable beam-splitter in an interferometer and as a calibrated attenuator for transmission measurements. These applications are discussed further in the following sections.

V. Measurement of Optical Constants

Refractive Index

The system used for the measurement of the refractive index of a sample is shown in Figure 9 . The output from the OPML, which is chopped to allow for lock-in detection, is first reflected through 90° by a wire-mesh reflector. A small portion of the output passes through the mesh reflector and is monitored by the detector, D_1. The primary beam then passes through a 20 cm. focal-length lens which produces a mildy convergent beam (half angle $\sim 4°$). This beam is divided by the dielectric prism coupler (DPC) described above. The transmitted beam traverses a mechanical phase shifter before coming to focus, while the reflected beam comes to focus at the sample S. The beam waist at sample has a radius $\omega_o = 0.6$ cm and a confocal length $z_o = 9.2$ cm, so the depth of focus is considerable. As the beams exit the phase shifter and the sample, they enter dielectric tubes which serve as low-loss transmission lines. After propagating through these tubes, the beams are allowed to expand for a short distance in free space before they are combined by a mylar-film beam-splitter (BS_2). The combined beams are then focused onto a Golay cell detector (D_2). The detector signal is sent to a lock-in amplifier and displayed on a chart recorder. A He - Ne laser (AL) in the other arm of the interferometer is aligned with the sample beam and used to orient the sample. The sample mount provides for rotation about a horizontal or a vertical axis and is on a rack and pinion drive for reproducible insertion or removal of the sample.

The first stage of the measurement procedure is to insert the sample, adjust the DPC to equalize the beam intensity at D_2 and adjust the phase

shifter to obtain an interference minimum. The sample is then removed and the phase shifter advanced until a new interference minimum is obtained. Letting L represent the net path change produced by the phase shifter, the index is calculated as $n = 1 + \frac{2N\pi + L}{d} + \frac{\delta\lambda_o}{2\pi d}$ where N is an integer, d the sample thickness, λ_o the vacuum wavelength and δ is a phaseshift which arises from the effects of multiple reflections in the sample (16). This term is usually quite small, but for high-index materials and certain values of d it can be substantial (See Section VI). The precise calculations of δ requires a knowledge of the absorption coefficient, which is determined in a separate measurement. The integer N can be found if an approximate value of the index is available, otherwise measurements on two samples of different thicknesses are necessary to determine N.

Table 2 shows the results obtained for several materials including: Rexolite and TPX plastics, and fused silica (Dynasil 4000). Results of other investigators are shown for comparison where available.

Absorption Coefficient

The system described above requires only minor modification to be used for measuring the transmission of a sample. The last beamsplitter (BS_2), the Golay cell, (D_2) and the alignment laser are removed. This gives access to the two beams from the DPC. Two identical pyroelectric detectors (described previously) are placed to intercept these two beams. Their outputs are fed to a ratiometer which displays the ratio of the power in the sample beam to the power in the other beam, which now serves as a reference. To perform a transmission measurement, the DPC is adjusted to produce a reading of one on the ratiometer, i.e. the two beams are equalized. The sample is then inserted and the new ratio is read. Assuming the detector and ratio-

meter have linear response, this ratio is directly the transmission of the sample.

There is an alternative method of determining the transmission which is less dependent upon detector and ratiometer linearity. In this method the DPC is used as a variable attenuator. After the sample has been inserted, the DPC is adjusted to restore a ratiometer reading of one and the travel of the DPC is noted. By referring to the calibration curve for the DPC (Figure 8), the power transmitted by the sample can be determined. This method is more tedious and is used only to confirm the results of the direct reading.

The relationship between the power transmission, T, and the optical constants of a material has been derived by several authors (17), (18). For the case of radiation which is normally incident on a plane, parallel plate of thickness d, the transmission can be expressed as

$$T = \frac{\rho(1 - R)^2 / R}{1 + \rho^2 - 2\rho \cos(2\varphi)} \quad \text{where}$$

$$R = \frac{(n - 1)^2}{(n + 1)^2}, \quad \rho = R \exp(-\alpha d), \quad \varphi = \frac{2\pi n d}{\lambda_o},$$

and α is the power absorption coefficient which we desire to determine.

This expression incorporates the effects of multiple reflections within the lamellar sample, however, for very lossy samples, corrections must be applied to include a small phase shift upon reflection and a slight enhancement of R.

The above result can be solved algebraically to obtain the parameter ρ in terms of the sample's transmission, index, and thickness. The result is $\rho = b - (b^2 - 1)^{\frac{1}{2}}$ where $b = (1 - R)^2/2RT + \cos(2\varphi)$. The power absorption coefficient is then given by $\alpha = \frac{-\ln(\rho/R)}{d}$. Calculation of α from the measured transmission in this manner requires an accurate knowledge of the sample's index and thickness. This is discussed further in Section VI.

Results obtained for Rexolite, TPX, and fused silica are shown in Table 2. Values obtained by other researchers are shown for comparison.

VI. Discussion of Errors

Refractive Index

The significant sources of error in the refractive index are the uncertainties in the sample thickness, Δd, and the phase shifter path-length change, ΔL. In terms of these quantities the error in the index, Δn, can be expressed as

$$\Delta n = \frac{1}{d}\left[(\Delta L)^2 + (n-1)^2 (\Delta d)^2\right]^{\frac{1}{2}}$$

The errors quoted in Table 2 were computed from this expression using the standard errors estimated for d and L. The thickest available samples were used to take advantage of the inverse dependence of the error on d.

The phase angle due to multiple reflections was computed from $\delta = \mathrm{Tan}^{-1}\left[\frac{\rho \sin 2\varphi}{1 - \rho \cos 2\varphi}\right]$, where ρ and φ are as defined in Section V. For the results reported here, the maximum contribution of this term to the index was *0.0003. Uncertainties in this small contribution were negligible.*

Absorption Coefficient

From the expression for α given in Section V, it is clear that the error in α depends not only upon the uncertainty in the measured transmission, ΔT, but also upon the uncertainties, Δn and Δd, in the sample's index and thickness. The expression for $\Delta\alpha$ in terms of these quantities is rather involved so a computer program was written to carry out the appropriate calculations and obtain $\Delta\alpha$ from estimates of ΔT, Δn, and Δd. Standard errors were used throughout.

The dominant term in $\Delta\alpha$ was found to be a periodic function of the form $\sin 2\varphi$. This is illustrated in Figure 10 which shows the expected total error in α, $\Delta\alpha$, for a small range of sample thickness about 1 cm. Values of $n = 2$ and $\alpha = 0.2$ were used for this plot and the uncertainties were assumed to be $\Delta T = 0.01$, $\Delta n = .001$, and $\Delta d = .0005$ cm. The periodic dependence of $\Delta\alpha$ on d

is quite pronounced, thus small changes in sample thickness can have a considerable effect on the error in α. Sample thicknesses which are a multiple of $\lambda/4$, where $\lambda = \frac{\lambda_o}{n}$, minimize the rate of change of α with n and d. These "good" thickness values include both the values for maximum reflection from the sample (even multiples of $\lambda/4$) and the values for minimum reflection (odd multiples of $\lambda/4$). Thicknesses which are an odd multiple of $\lambda/8$ correspond to the maximum rate of change of α with n and d and should be avoided. Judicious choices of sample thickness can result in a reduced dependence of α on sample index and thickness. This is especially important in the case of samples with a large refractive index and low absorption.

VII. Conclusion

We have demonstrated that a double-beam, quasi-optical system which is simple to assemble and operate can yield high precision measurements of optical constants in the NMM region when a laser source is used. Extension of these measurements in frequency by use of other laser lines is currently in progress.

Modification which will further reduce the measurement errors are planned. In this measurement of refractive index, the predominant error source is the uncertainty in L which arises from the manual procedure used to locate the interference minima. Automation of this procedure with a computerized data collection system is planned to reduce this uncertainty.

As noted in Section VI, the uncertainty in the determination of the absorption coefficient is a sensitive function of the sample thickness. More extensive sample preparation and gauging is planned to allow optimization of this factor.

The performance of this system is under evaluation with a variety of samples, e.g. high-index and/or high-loss materials. Future studies will concentrate on materials with potential for device application including semiconductors, ferrites and ferroelectrics.

References

1. T. Y. Chang and T. J. Bridges, Opt. Commun. 1, 423 (1970).

2. M. Yamanaka, J. Opt. Soc. Amer., 67, 952 (1977).

3. D. T. Hodges, F. B. Foote, and R. D. Reel, IEEE J. Quantum Electron., QE-13, 491 (1977).

4. A. Yariv, Quantum Electronics, Second Edition, John Wiley and Sons, Inc., New York, N. Y. (1975).

5. D. J. E. Knight, NPL Report No. QU45, 1982.

6. E. A. J. Marcatili and R. A. Schmeltzer, Bell System Tech. J., 43, 1783 (1964).

7. H. Steffen and F. K. Kneubühl, Phys. Lett., 27A, 612 (1968).

8. J. J. Degnan, Appl. Opt., 12, 1026 (1973).

9. R. L. Abrams, IEEE J. Quantum Electron., QE-8, 838 (1972).

10. J. P. Creen, IEEE MTT-27, 573 (1979).

11. P. Belland and J. P. Crenn, Appl. Opt., 21, 522 (1982).

12. R. G. Fellers, Proc. IEEE, 55, 1003 (1967).

13. J. J. Taub, H. J. Hindin, O. F. Hinckelmann, and M. L. Wright, IEEE Trans on Microwave Th. and Tech., MTT-11, 238 (1963).

14. H. D. Raker and C. R. Valenzuela, IEEE Trans on Microwave Theory and Techniques MTT-10, 392 (1962).

15. R. G. Fellers and J. Taylor, IEEE Trans. on Microwave Theory and Techniques, MTT-12, 584 (1964).

16. G. R. Fowles, Introduction to Modern Optics, Holt, Rinehart and Winston, Inc., pp. 68-88 (1975).

17. E. E. Bell, Handbuch der Physik, Bd. XXV/2a.

18. C. M. Randall and R. D. Rawcliffe, Applied Optics, 6, 1889 (1967).

19. G. J. Simonis, Private Communication.

20. G. J. Simonis, and R. D. Felock, Applied Optics, 22, 194 (1983).

21. J. Chamberlain, J. Haigh and M. J. Hine, Infrared Phys., 11, 75 (1971).

22. R. C. Jones, J. of Phys. D: Appl. Phys., 9, 819 (1976).

Table 1

Laser Lines Between 150 GHz and 400 GHz

Wavelength (mm)	Frequency (GHz)	Molecule Used
1.965	153	MBA
1.887	159	MC
1.573	191	MBA
1.310	229	MBA
1.254	239	MI
1.222	245	MF13
1.063	282	MI
0.944	318	MC
0.925	324	MBA
0.871	344	MC
0.749	400	MBA
0.715	419	MBA

MBA = $CH_3^{79}Br$, methyl bromide; MC = CH_3Cl, methyl chloride;
MI = CH_3I, methyl iodide; MF13 = $^{13}CH_3F$, methyl flouride.

Table 2

EXPERIMENTAL RESULTS

MATERIAL	This Work at 245 GHz			Literature	
	Thickness	n	$\alpha(cm^{-1})$	n	$\alpha(cm^{-1})$
Rexolite[a] (1422)	56.137 mm.	1.5913 ± .0001	.170 ± .002	1.590 ± .002[19]	0.22[22]
TPX[b]	25.391 mm.	1.4576 ± .0001	0.047 ± .003	1.459 ± .001[20] 1.456 ± .002[21]	0.53[22]
Fused[c] Silica	9.990 mm.	1.955 ± .001	0.178 ± .009		

a. Polystyrene, cross linked (Obtained from C-LEC Plastics, Inc.).

b. Poly-4-methyl-pentene 1.

c. Dynasil 4000

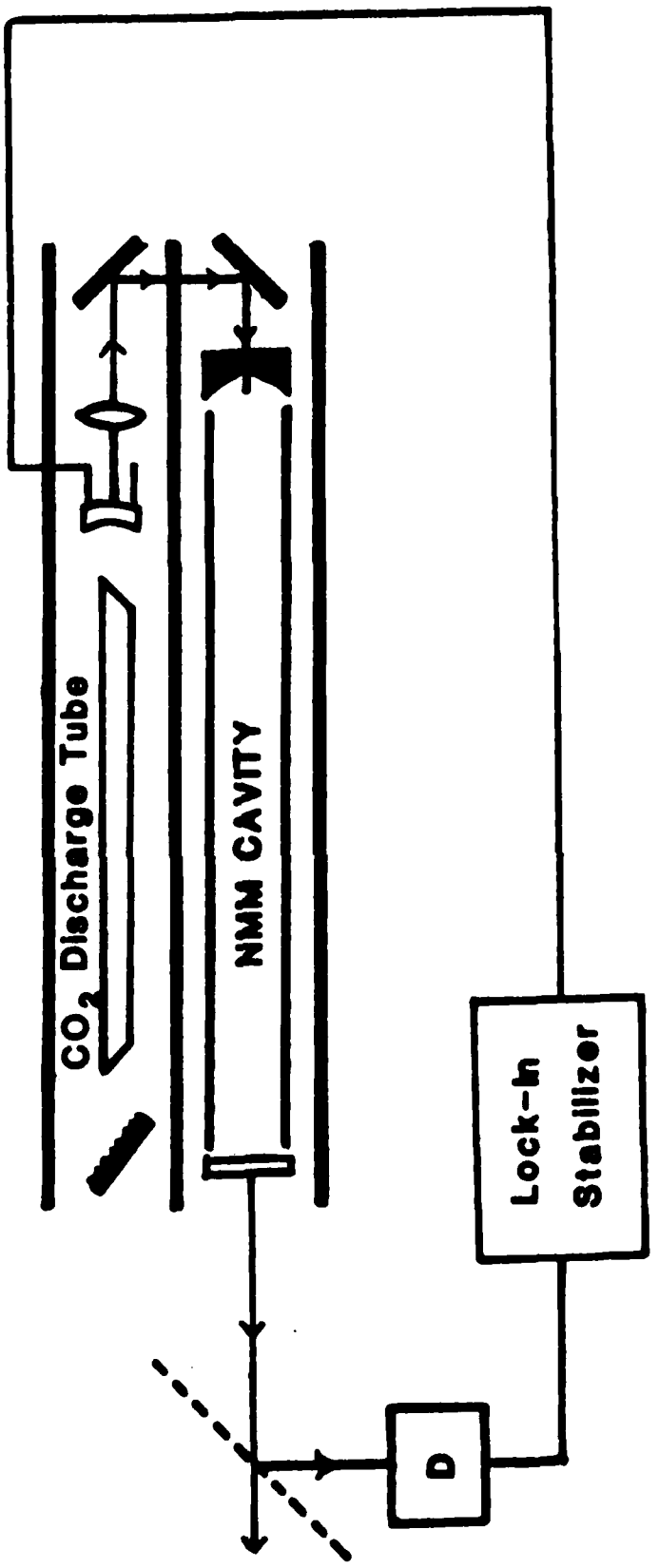

Figure 1. Optically pumped molecular laser system.

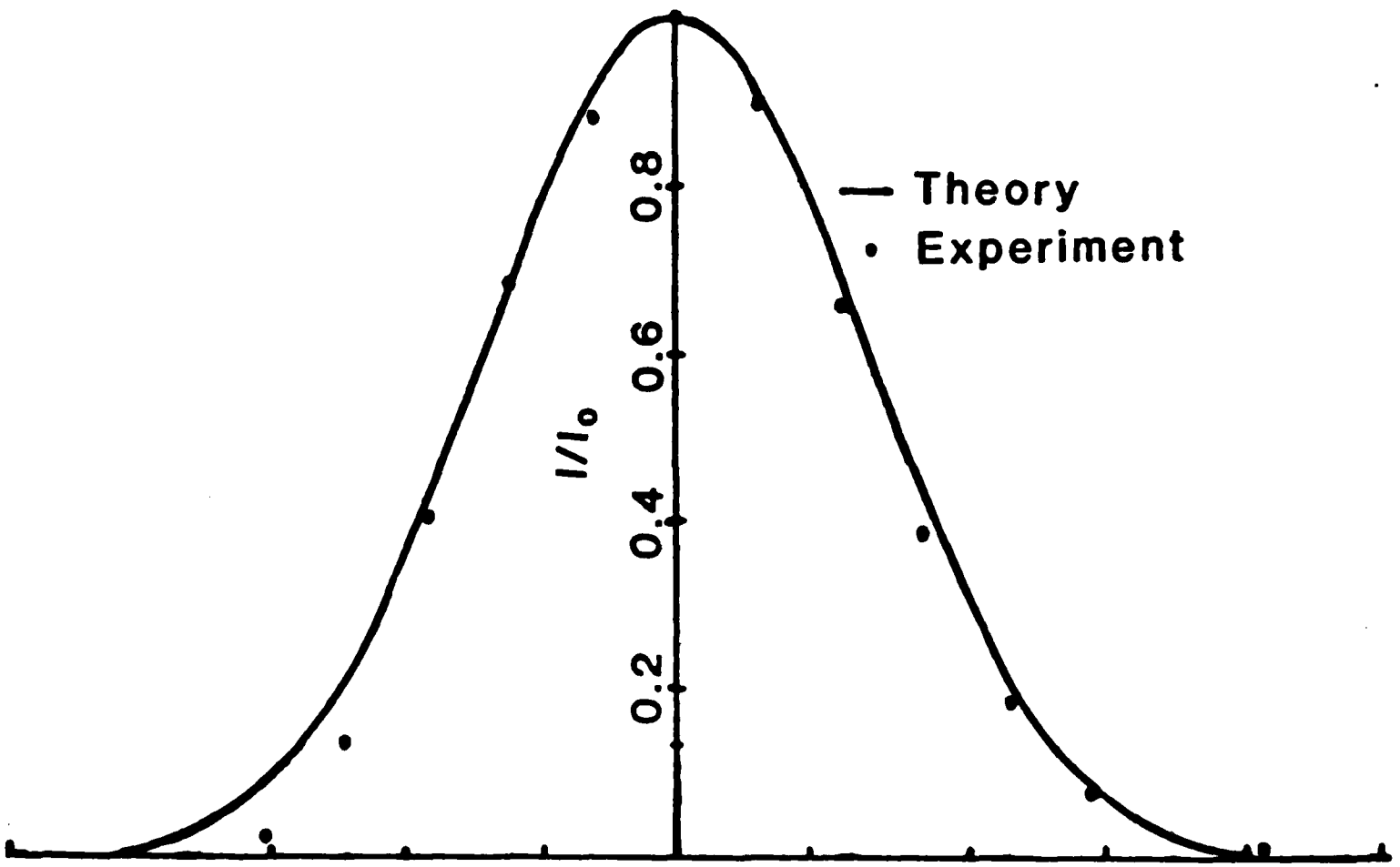

Figure 2. A typical beam profile of the optically pumped molecular laser focused output beam.

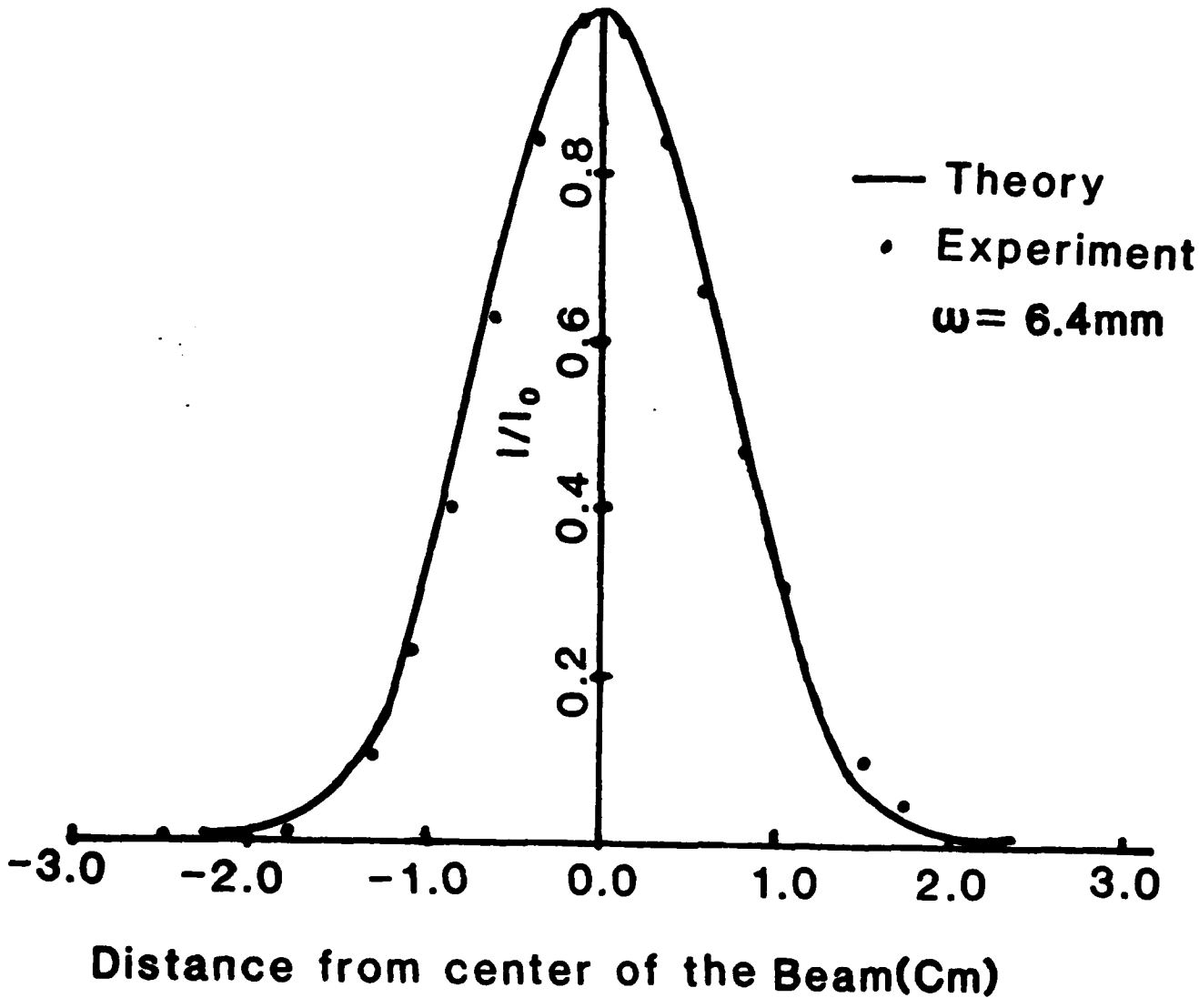

Figure 3. Intensity profile of EH_{11} mode launched from a 1 m long hollow dielectric waveguide of I.D. 0.95 cm at a distance of 20 cm.

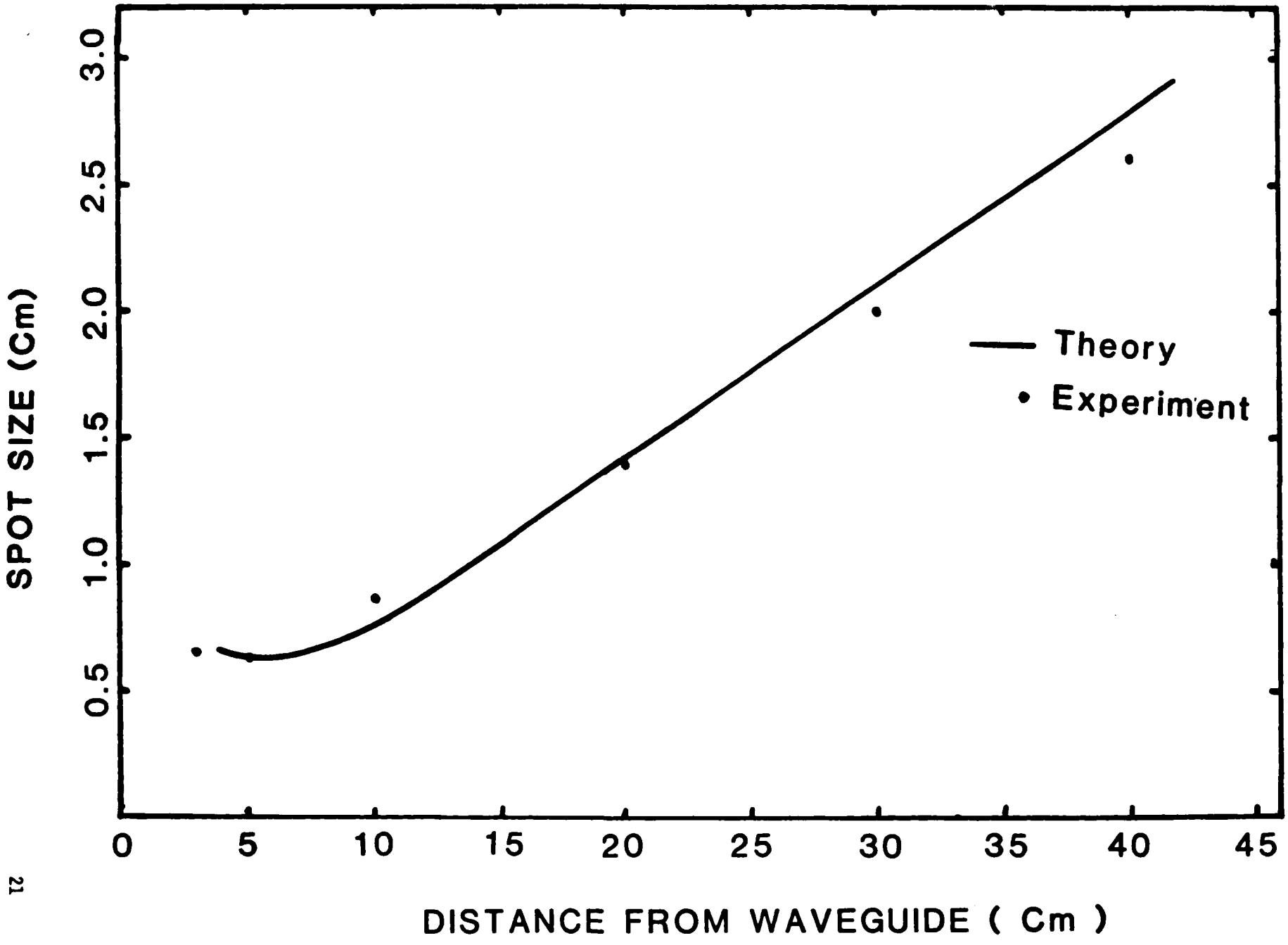

Figure 4. Expansion of the EH_{11} mode launched from a 1 m long hollow dielectric guide of 0.95 cm I.D.

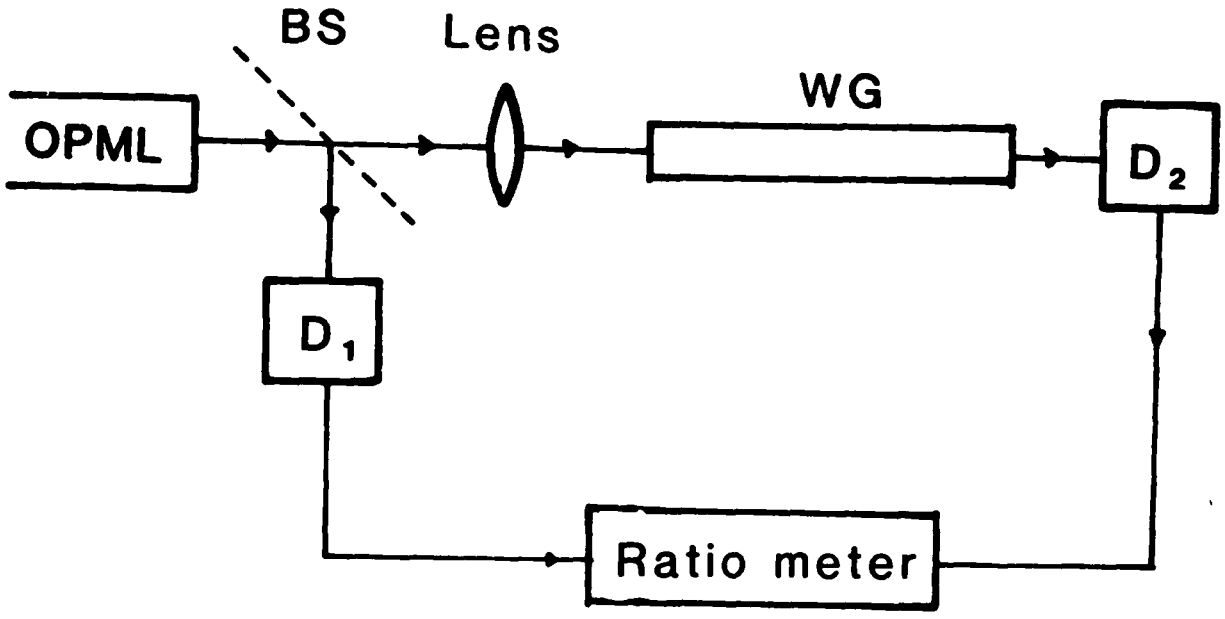

Figure 5. Block diagram of the experimental arrangement for the transmission measurement. D_1 and D_2, pyroelectric detectors (Laser Precision Rkp-545); ratiometer (Laser Precision Rkp-5200).

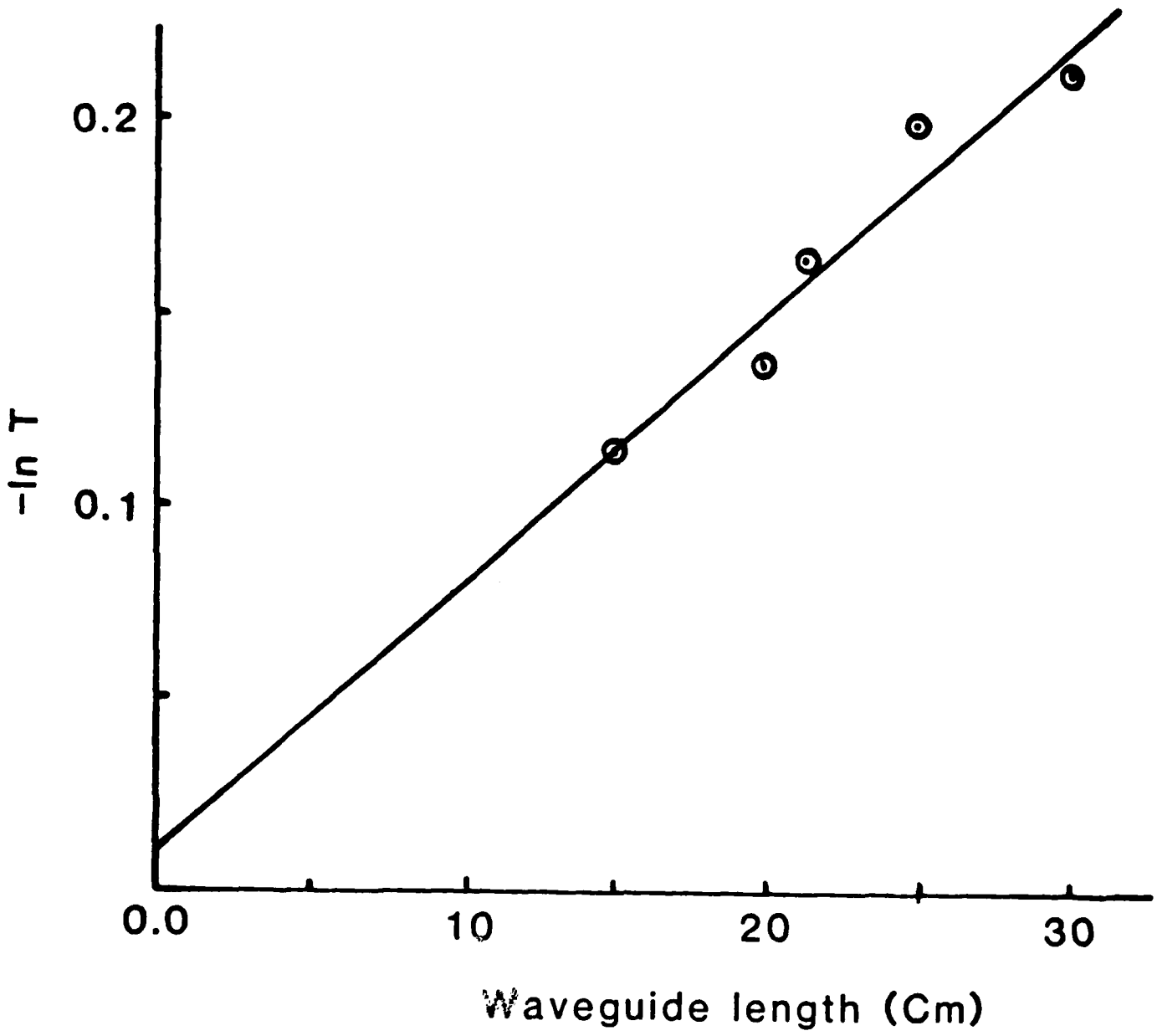

Figure 6. The attenuation of the low-loss EH_{11} mode in circular plexiglass tubes of I.D. 0.95 cm, and of various lengths. The measured value of the attenuation constant is $(6.97 \times 10^{-3} \pm 1.1 \times 10^{-3})$ cm^{-1}, whereas, the predicted value is 7.74×10^{-3} cm^{-1}. Measured coupling loss is $(1 \pm 2.4)\%$.

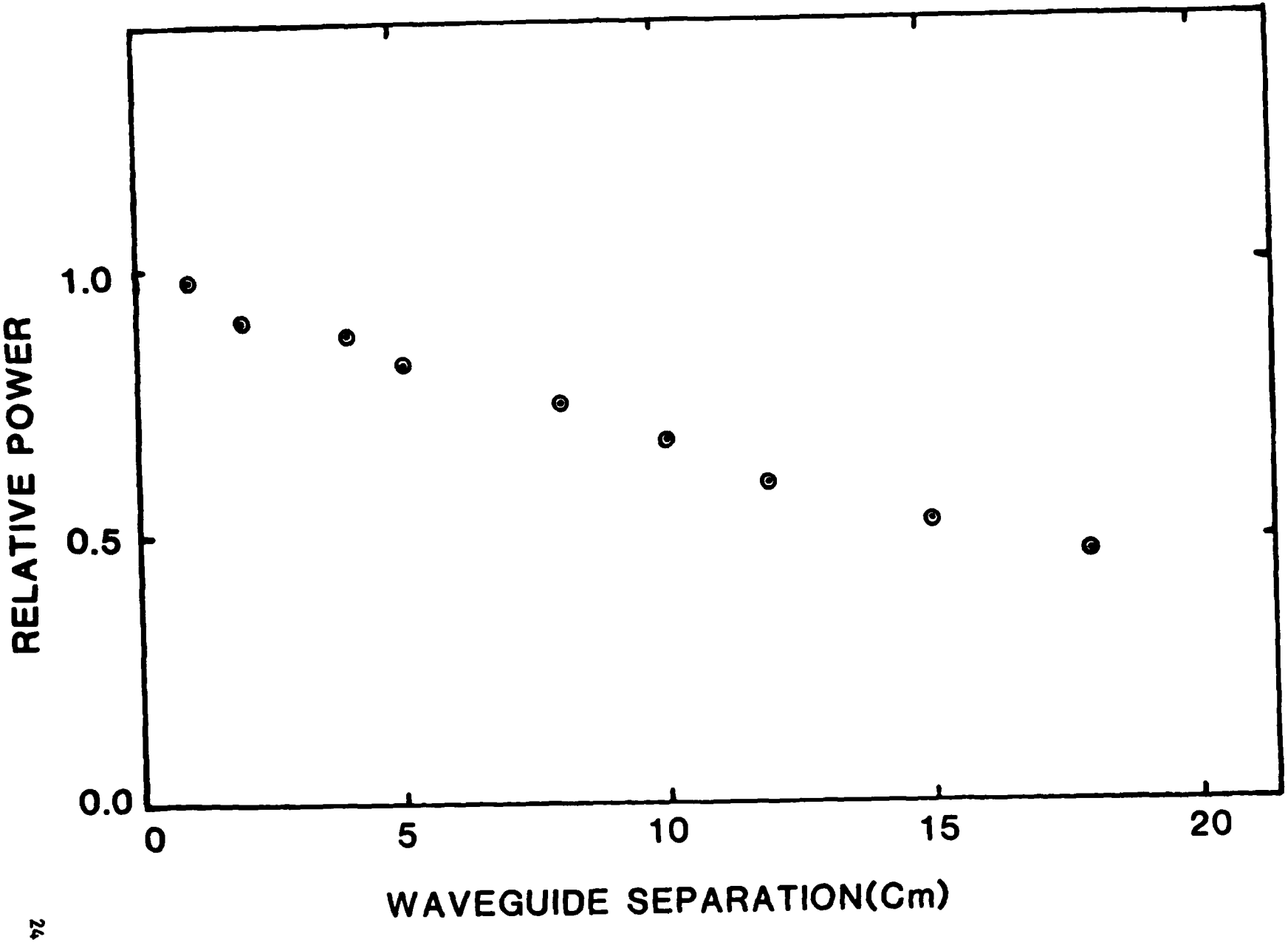

Figure 7. The relative power at the exit to the second guide versus the gap length between two guides.

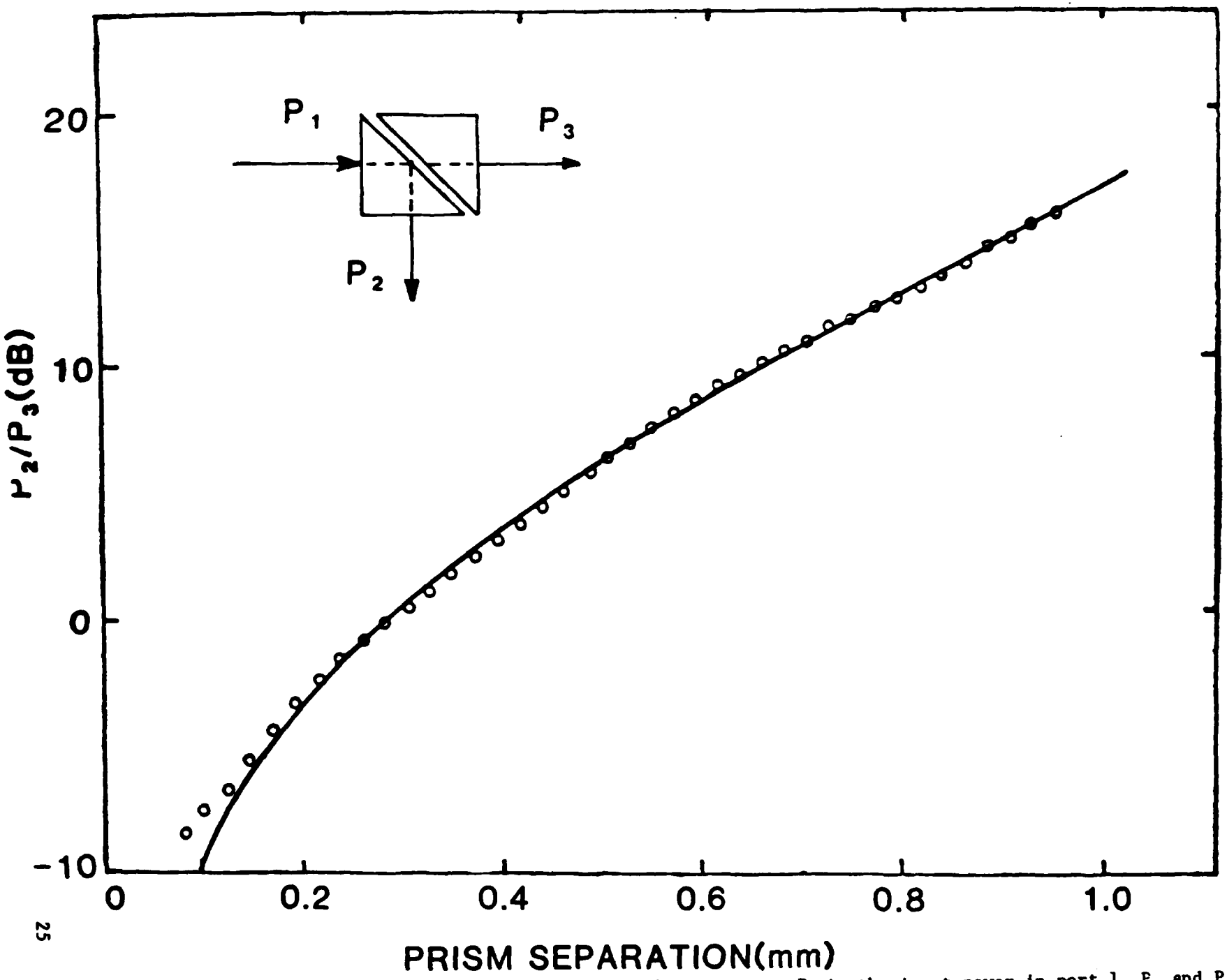

Figure 8. Top Left: Double-prism variable coupler/attenuator. P_1 is the input power in port 1, P_2 and P_3 are powers in ports 2 and 3 respectively. The curve is due to P_2/P_3 versus prism separation. The open circles are data points and the solid line is the theoretical fit (Ref. 12).

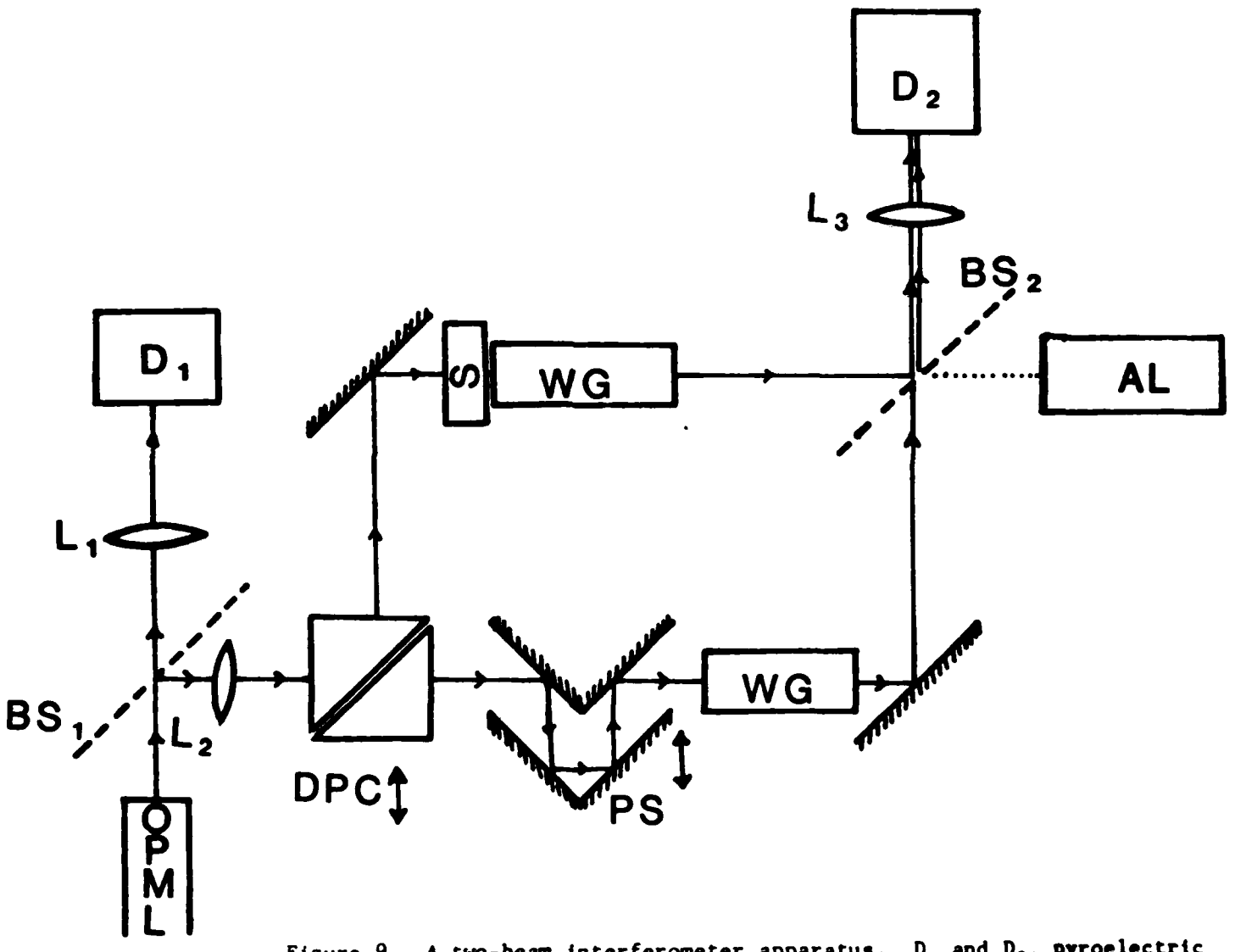

Figure 9. A two-beam interferometer apparatus. D_1 and D_2, pyroelectric detectors (Laser Precision Rkp-545): L_1, L, and L_3, TPx lens; BS_1, wire-mesh beam splitter; BS_2, mylar-film beam splitter; DPC, double-prism coupler; PS, phase shifter; S, sample holder; WG, dielectric waveguides; and AL, He-Ne alignment laser.

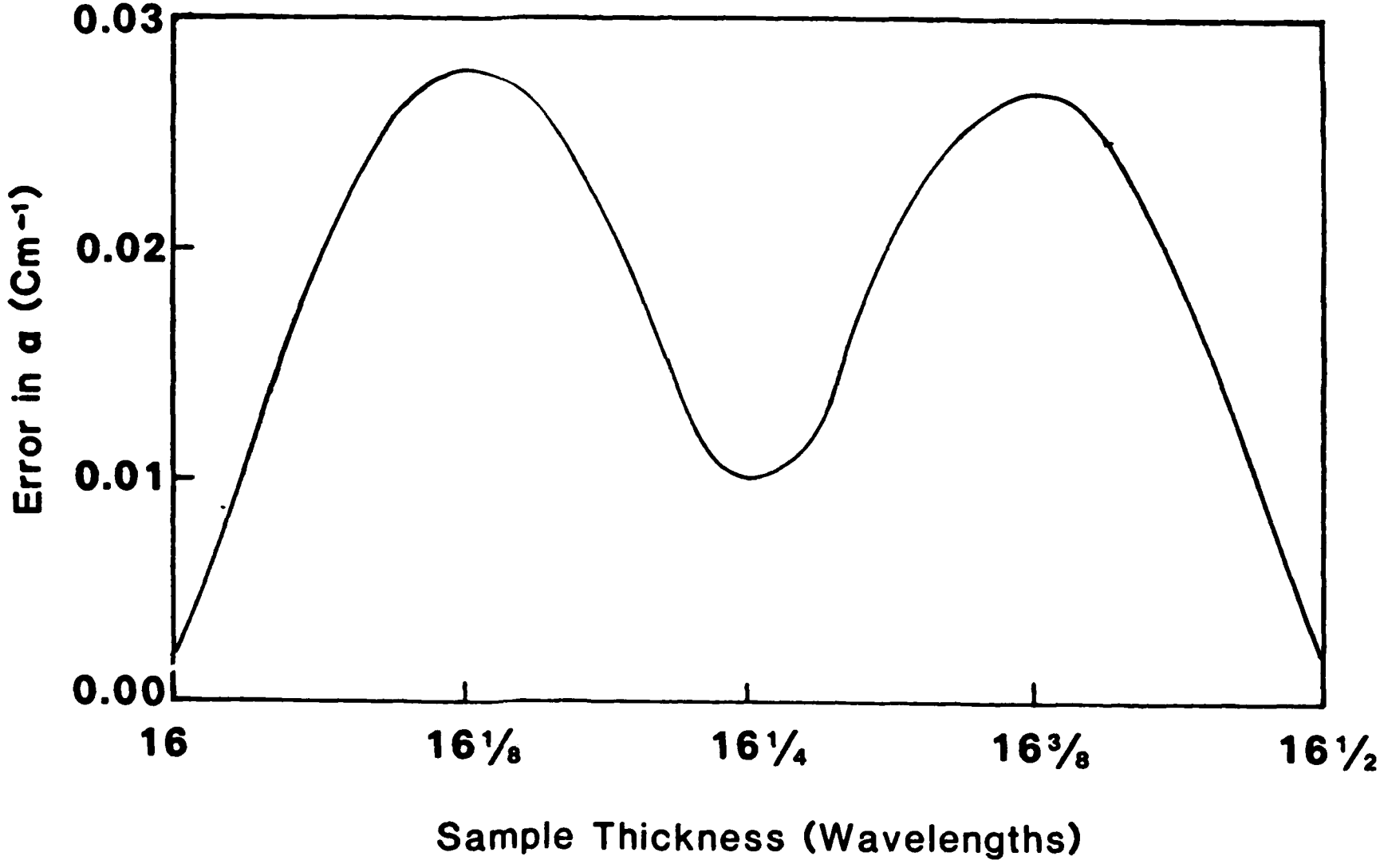

Figure 10. Total error in the absorption coefficient as a function of sample thickness.

PUBLICATION LIST

1. C. Ronald Jones, J. M. Dutta, and H. Dave, "Two-beam Interferometer for Optical Constants Measurements at Near Millimeter Wavelengths," (accepted for publication in Int. J. of IR and MM Waves, November issue, 1983).

2. J. M. Dutta, C. R. Jones, and H. Dave, "Optical Constant Measurements in Near-Millimeter Wavelength Region Using Quasi Optical Techniques, " Conf. Digest, Seventh Int. Conf. on IR and MM Waves, Feb. '83, Marseille, France

3. C. R. Jones and J. M. Dutta, "Tunable Sideband Generator for High Resolution Submillimeter Spectroscopy," Conf. Digest, Sixth Int. Conf. on IR and MM Waves, December '81, Miami Beach, Florida, USA.

PARTICIPATING SCIENTIFIC PERSONNEL

(1) Dr. Jyotsna M. Dutta, Co-Principal Investigator

(2) Dr. Charles R. Jones, Co-Principal Investigator

(3) Dr. Hemant Dave, Investigator

(4) Mr. Roland Adu-Poku, Research Assistant

(5) Mr. Benjamin Edwards, Research Assistant

(6) Ms. Marian Peters, Research Assistant


DAT
FILM